

## Elliptic and Triangular Flow in Event-by-Event $D = 3 + 1$ Viscous Hydrodynamics

Björn Schenke, Sangyong Jeon, and Charles Gale

*Department of Physics, McGill University, 3600 University Street, Montreal, Quebec, H3A 2T8, Canada*  
(Received 1 October 2010; published 27 January 2011)

We present results for the elliptic and triangular flow coefficients  $v_2$  and  $v_3$  in Au + Au collisions at  $\sqrt{s} = 200$  AGeV using event-by-event  $D = 3 + 1$  viscous hydrodynamic simulations. We study the effect of initial state fluctuations and finite viscosities on the flow coefficients  $v_2$  and  $v_3$  as functions of transverse momentum and pseudorapidity. Fluctuations are essential to reproduce the measured centrality dependence of elliptic flow. We argue that simultaneous measurements of  $v_2$  and  $v_3$  can determine  $\eta/s$  more precisely.

DOI: 10.1103/PhysRevLett.106.042301

PACS numbers: 12.38.Mh, 24.10.Nz, 25.75.Ld

Fluctuating initial conditions for hydrodynamic simulations of heavy-ion collisions have been argued to be very important for the exact determination of collective flow observables and to describe specific features of multiparticle correlation measurements in heavy-ion collisions at Brookhaven National Laboratory's Relativistic Heavy-Ion Collider (RHIC) [1–17]. Long-range correlations in pseudorapidity and double-peak structures on the away-side in  $\Delta\eta_p - \Delta\phi$  correlations have been reproduced using initial states with fluctuations in the transverse plane, extending as flux tubes along the beam line [11–13,16].

In this work we report on results for both elliptic and triangular flow obtained with an event-by-event  $D = 3 + 1$  relativistic hydrodynamic simulation, an extension of MUSIC [18], including shear viscosity. We first briefly describe the inclusion of viscosity and leave a more detailed description to a forthcoming work.

In the first-order formalism for viscous hydrodynamics, the stress-energy tensor is decomposed into

$$T_{\text{1st}}^{\mu\nu} = T_{\text{id}}^{\mu\nu} + S^{\mu\nu}, \quad (1)$$

where

$$T_{\text{id}}^{\mu\nu} = (\epsilon + \mathcal{P})u^\mu u^\nu - \mathcal{P}g^{\mu\nu} \quad (2)$$

is the ideal fluid part with flow velocity  $u^\mu$ , local energy density  $\epsilon$  and local pressure  $\mathcal{P}$ . The flow velocity is defined as the timelike eigenvector of  $T_{\text{id}}^{\mu\nu}$ ,  $T_{\text{id}}^{\mu\nu}u_\nu = \epsilon u^\mu$ , with the normalization  $u^\nu u_\nu = 1$  and the pressure is determined by the equation of state as a function of  $\epsilon$ .

The viscous part of the stress-energy tensor in the first-order approach is given by

$$S^{\mu\nu} = \eta \left( \nabla^\mu u^\nu + \nabla^\nu u^\mu - \frac{2}{3} \Delta^{\mu\nu} \nabla_\alpha u^\alpha \right) \quad (3)$$

where  $\Delta^{\mu\nu} = g^{\mu\nu} - u^\mu u^\nu$  is the local 3-metric and  $\nabla^\mu = \Delta^{\mu\nu} \partial_\nu$  is the local space derivative. Note that  $S^{\mu\nu}$  is transverse with respect to the flow velocity since  $\Delta^{\mu\nu} u_\nu = 0$  and  $u^\nu u_\nu = 1$ . Hence,  $u^\mu$  is also an eigenvector of the whole stress-energy tensor with the same eigenvalue  $\epsilon$ .

This form of viscous hydrodynamics is conceptually simple. However, this Navier-Stokes form is known to introduce unphysical superluminal signals. There are several remedies for this problem [19–23], all of them employing the second order formalism. In this work, we use a variant of the Israel-Stewart formalism derived in [24], where the stress-energy tensor is decomposed as

$$\mathcal{T}^{\mu\nu} = T_{\text{id}}^{\mu\nu} + W^{\mu\nu}. \quad (4)$$

The evolution equations are  $\partial_\mu \mathcal{T}^{\mu\nu} = 0$  and

$$\Delta_\alpha^\mu \Delta_\beta^\nu u^\sigma \partial_\sigma W^{\alpha\beta} = -\frac{1}{\tau_\pi} (W^{\mu\nu} - S^{\mu\nu}) - \frac{4}{3} W^{\mu\nu} (\partial_\alpha u^\alpha). \quad (5)$$

In the  $\tau, \eta_s$  coordinate system we use, these equations can be rewritten as hyperbolic equations with sources

$$\partial_a T_{\text{id}}^{ab} = -\partial_a W^{ab} + F^b \quad (6)$$

and

$$\partial_a (u^a W^{cd}) = -(1/\tau_\pi)(W^{cd} - S^{cd}) + G^{cd} \quad (7)$$

where  $F^b$  and  $G^{cd}$  contain terms introduced by the coordinate change from  $t, z$  to  $\tau, \eta_s$  as well as those introduced by the projections in Eq. (5).

Our approach to solve these hyperbolic equations relies on the Kurganov-Tadmor scheme [25,26]. See [18] for details. As opposed to the ideal case described in [18], we now face time derivatives in the source term. These are handled with the first-order approximation  $\dot{g}(\tau_n) = (g(\tau_n) - g(\tau_{n-1}))/\Delta\tau$  in the first step of the Heun method, and in the second step we use  $\dot{g}(\tau_n) = (g^*(\tau_{n+1}) - g(\tau_n))/\Delta\tau$  where  $g^*(\tau_{n+1})$  is the result from the first step.

As most Eulerian algorithms, ours suffers from numerical instability when the density becomes small while the flow velocity becomes large. Fortunately this happens late in the evolution of the system. Regularizing such instability has no strong effects on the observables we are interested in. Some ways of handling this are known (see,

e.g., Ref. [27]). Setting the local viscosity to zero when finite viscosity causes negative pressure in the cell as advocated in [27] and reducing the ideal part by 5% works well to stabilize the calculations without introducing spurious effects.

While in standard hydrodynamic simulations with averaged initial conditions all odd flow coefficients vanish by definition, fluctuations generate triangular flow  $v_3$  as a response to the finite initial triangularity. We follow [17] and define an event plane through the angle

$$\psi_n = \frac{1}{n} \arctan \frac{\langle p_T \sin(n\phi) \rangle}{\langle p_T \cos(n\phi) \rangle}, \quad (8)$$

where the weight  $p_T$  is chosen for best accuracy [28]. Then, the flow coefficients can be computed using

$$v_n = \langle \cos[n(\phi - \psi_n)] \rangle. \quad (9)$$

The initialization of the energy density is done using a Glauber Monte Carlo model (see [29]): Before the collision the density distribution of the two nuclei is described by a Woods-Saxon parametrization, which we sample to determine the positions of individual nucleons. The impact parameter is sampled from the distribution  $P(b)db = 2bdb/(b_{\max}^2 - b_{\min}^2)$ , where  $b_{\min}$  and  $b_{\max}$  depend on the given centrality class. Two nucleons are assumed to collide if their relative transverse distance is less than  $D = \sqrt{\sigma_{NN}/\pi}$ , where  $\sigma_{NN}$  is the inelastic nucleon-nucleon cross section, which at top RHIC energy of  $\sqrt{s} = 200$  AGeV is  $\sigma_{NN} = 42$  mb. The energy density is distributed proportionally to the wounded nucleon distribution. For every wounded nucleon we add a contribution to the energy density with Gaussian shape (in  $x$  and  $y$ ) and width  $\sigma_0 = 0.4$  fm. Using  $\sigma_0 = 0.8$  fm reduces both  $v_2$  and  $v_3$  on average by  $\sim 8\%$  and produces steeper transverse momentum spectra for  $p_T > 2$  GeV (also see [15]). We will study a finite contribution from binary collision scaling, which can increase the average initial eccentricity, in a future work. In the rapidity direction, we assume the energy density to be constant on a central plateau and fall like half-Gaussians at large  $|\eta_s|$  (see [18]). This procedure generates flux-tube-like structures compatible with measured long-range rapidity correlations [30–32]. The absolute normalization is determined by demanding that

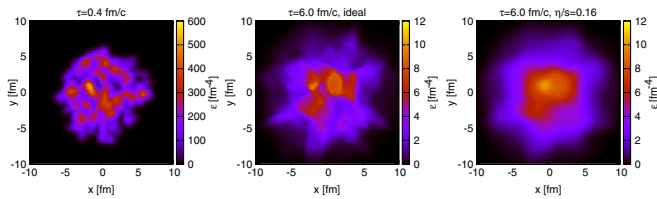


FIG. 1 (color online). Energy density distribution in the transverse plane for one event with  $b = 2.4$  fm at the initial time (left), and after  $\tau = 6$  fm/c for the ideal case (middle) and with  $\eta/s = 0.16$  (right).

the obtained total multiplicity distribution reproduces the experimental data. We will present a more detailed study of particle spectra and dependencies on different parameters in a forthcoming work. See [18] for details on parameter sets and obtained particle spectra in the ideal case with average initial conditions. As equation of state we employ the parametrization “s95p-v1” from [33], obtained from interpolating between lattice data and a hadron resonance gas.

In Fig. 1 we show the energy density distribution in the transverse plane for an event with impact parameter  $b = 2.4$  fm at the initial time  $\tau_0 = 0.4$  fm/c and at time  $\tau = 6$  fm/c for  $\eta/s = 0$  and  $\eta/s = 0.16$ . This clearly shows the effect of dissipation.

We perform a Cooper-Frye freeze-out using

$$E \frac{dN}{d^3p} = \frac{dN}{dy p_T dp_T d\phi_p} = g_i \int_{\Sigma} f(u^\mu p_\mu) p^\mu d^3\Sigma_\mu, \quad (10)$$

where  $g_i$  is the degeneracy of particle species  $i$ , and  $\Sigma$  the freeze-out hypersurface. In the ideal case the distribution function is given by

$$f(u^\mu p_\mu) = f_0(u^\mu p_\mu) = \frac{1}{(2\pi)^3} \frac{1}{\exp[(u^\mu p_\mu - \mu_i)/T_{FO}] \pm 1}, \quad (11)$$

where  $\mu_i$  is the chemical potential for particle species  $i$  and  $T_{FO}$  is the freeze-out temperature. In the finite viscosity case we include viscous corrections to the distribution function,  $f = f_0 + \delta f$ , with

$$\delta f = f_0(1 \pm f_0) p^\alpha p^\beta W_{\alpha\beta} \frac{1}{2(\epsilon + \mathcal{P})T^2}, \quad (12)$$

where  $W$  is the viscous correction introduced in Eq. (4). Note that the choice  $\delta f \sim p^2$  is not unique [34]. We use fixed freeze-out energy densities of  $0.12$  GeV/fm<sup>3</sup> and  $0.16$  GeV/fm<sup>3</sup>, corresponding to  $T_{FO} = 136$  MeV and  $142$  MeV for ideal and viscous calculations, respectively.

The algorithm used to determine the freeze-out surface  $\Sigma$  [18] is very efficient in determining the freeze-out

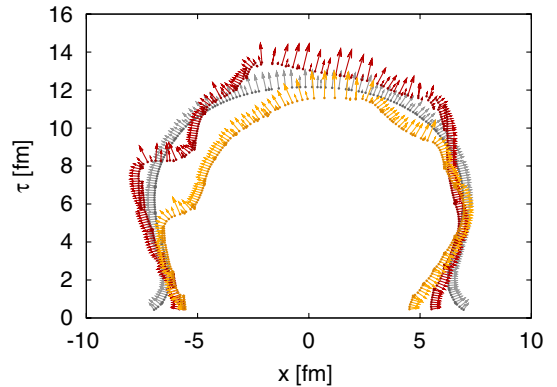


FIG. 2 (color online). Freeze-out surfaces for two different events (red [dark gray] and yellow [medium gray]) compared to that for the averaged initial condition (light gray).

surface of a system with fluctuating initial conditions. We demonstrate this in Fig. 2, where we show freeze-out surface in the  $x$ - $\tau$  plane in the vicinity of  $y = 0$  fm and  $\eta_s = 0$  for two different initial distributions compared to that for an averaged initial condition. The arrows are projections of the normal vector on the hypersurface element onto the  $x$ - $\tau$  plane.

We include resonances up to the  $\phi$  meson. The pseudorapidity dependence of both  $v_2$  and  $v_3$  is affected notably by the inclusion of resonance decays, improving the agreement of  $v_2(\eta_p)$  with data significantly.  $v_2(p_T)$  at midrapidity is almost unaffected by the resonances while  $v_3(p_T)$  is reduced by approximately 20%–30%. Flow observables have been shown to depend mainly on these lower resonances [35,36] such that it is a good approximation to omit contributions from resonances above the  $\phi$  meson. Average  $p_T$  in most central collisions are approximately 0.53 GeV for all studied viscosities.

Figure 3 shows the elliptic flow  $v_2$  for charged hadrons as a function of transverse momentum obtained from an averaged initial condition in the ideal case and for an average over 100 individual events for  $\eta/s \in \{0, 0.08, 0.16\}$ . We compare to data from STAR [37] and PHENIX [38].

Shaded bands indicate statistical errors. While in the most central collisions fluctuations increase  $v_2$  compared to the case with averaged initial conditions, for 10%–20% central collisions the difference is negligible and for 30%–40% central collisions fluctuations reduce the elliptic flow. The increase for central collisions is easy to understand.

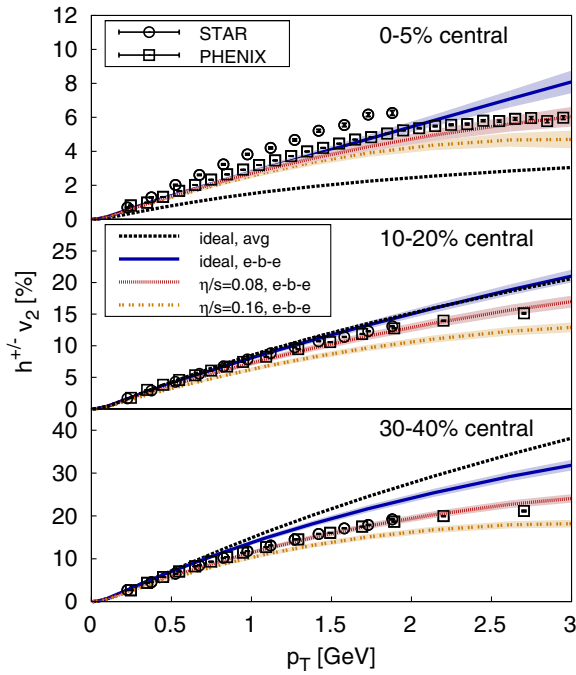


FIG. 3 (color online). Charged hadron  $v_2$  for different centralities as a function of  $p_T$  for averaged initial conditions (avg) and event-by-event simulations (e-b-e) using different  $\eta/s$  compared to STAR [37] and PHENIX [38] data.

Single events have a larger anisotropy with respect to the event plane than the average with respect to the reaction plane, hence increasing the obtained  $v_2$ . This effect decreases with increasing centrality eventually making the event-by-event  $v_2$  smaller compared to the averaged initial condition case. This can be understood by the fact that for more peripheral collisions, individual hot spots with a more isotropic shape influence the expansion. Given these effects, we conclude that evolving single events and averaging the final result has a clear effect on the centrality dependence of  $v_2$ .

Viscosity reduces the elliptic flow for all centralities as also found in (2 + 1)-dimensional simulations [39–42].

Triangular flow  $v_3$  as a function of  $p_T$  is shown in Fig. 4.  $v_3$  depends less strongly on the centrality than  $v_2$  since it is completely fluctuation driven. It is largest for an ideal fluid and reduces similarly to  $v_2$  with increasing viscosity of the medium.

The upper panel of Fig. 5 shows the pseudorapidity dependence of  $v_2$  for 15%–25% central collisions compared to PHOBOS data [43]. A reduction of elliptic flow with increasing viscosity is visible, particularly for large pseudorapidities  $|\eta_p|$ , which has been anticipated [18,44]. The results indicate that  $\eta/s$  grows towards large  $|\eta_p|$ , which is expected because of the less dense system in that region. However, there could be other reasons for the disagreement, such as longitudinal fluctuations or modified decoupling at higher rapidities. Hadronic rescattering within a hadron cascade model can also improve the agreement with experimental data [45]. In the lower panel of

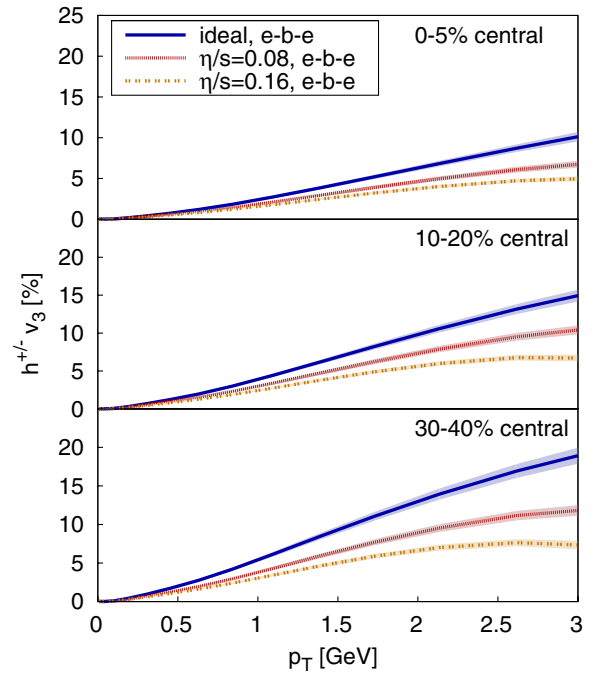


FIG. 4 (color online). Charged hadron  $v_3$  for different centralities as a function of  $p_T$  for event-by-event simulations using different viscosity to entropy density ratios.

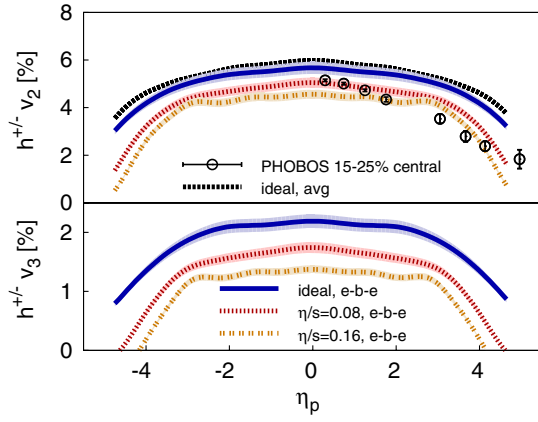


FIG. 5 (color online). Charged hadron  $v_2$  and  $v_3$  as a function of pseudorapidity for event-by-event simulations using different viscosity to entropy density ratios.

Fig. 5 we present the  $\eta_p$  dependence of  $v_3$ . Again, the decrease of  $v_3$  with increasing viscosity is visible, being strongest for large  $|\eta_p|$ .

We presented the elliptic and triangular flow coefficients obtained with an event-by-event analysis using (3 + 1)-dimensional relativistic viscous hydrodynamics. Charged hadron elliptic flow around midrapidity is well described for a wide range of centralities when using  $\eta/s = 0.08$ , the conjectured lower bound from anti-de Sitter/conformal field theory correspondence [46]. A similarly small value was found in a parton cascade model based on perturbative QCD [47]. Larger viscosities underestimate elliptic flow. Shear viscosity reduces  $v_2$  especially for larger pseudorapidities; however, the data cannot be described for all  $\eta_p$  when using constant  $\eta/s$ . Triangular flow has a weaker dependence on centrality. We determined its  $p_T$  and  $\eta_p$  dependence and its dependence on  $\eta/s$ . When  $v_3$  data becomes available, combined analyses of both  $v_2$  and  $v_3$  can make an accurate determination of the shear viscosity possible.

We thank Pasi Huovinen and Paul Romatschke for helpful comments and Todd Springer for fruitful discussions and checks. This work was supported in part by the Natural Sciences and Engineering Research Council of Canada. B.P.S. gratefully acknowledges a Richard H. Tomlinson grant by McGill University.

[1] R. Andrade *et al.*, *Phys. Rev. Lett.* **97**, 202302 (2006).  
 [2] A. Adare *et al.*, *Phys. Rev. C* **78**, 014901 (2008).  
 [3] B.I. Abelev *et al.*, *Phys. Rev. Lett.* **102**, 052302 (2009).  
 [4] B. Alver *et al.*, *Phys. Rev. C* **81**, 024904 (2010).  
 [5] B. Alver *et al.*, *Phys. Rev. Lett.* **104**, 062301 (2010).  
 [6] B.I. Abelev *et al.*, *Phys. Rev. C* **80**, 064912 (2009).  
 [7] M. Miller and R. Snellings, arXiv:nuclex/0312008.

[8] W. Broniowski, P. Bozek, and M. Rybczynski, *Phys. Rev. C* **76**, 054905 (2007).  
 [9] R. Andrade *et al.*, *Phys. Rev. Lett.* **101**, 112301 (2008).  
 [10] T. Hirano and Y. Nara, *Nucl. Phys. A* **830**, 191c (2009).  
 [11] J. Takahashi *et al.*, *Phys. Rev. Lett.* **103**, 242301 (2009).  
 [12] R. Andrade *et al.*, *J. Phys. G* **37**, 094043 (2010).  
 [13] B. Alver and G. Roland, *Phys. Rev. C* **81**, 054905 (2010).  
 [14] K. Werner *et al.*, *Phys. Rev. C* **82**, 044904 (2010).  
 [15] H. Holopainen, H. Niemi, and K.J. Eskola, arXiv:1007.0368.  
 [16] B. Alver *et al.*, *Phys. Rev. C* **82**, 034913 (2010).  
 [17] H. Petersen, G.-Y. Qin, S. A. Bass, and B. Muller, *Phys. Rev. C* **82**, 041901 (2010).  
 [18] B. Schenke, S. Jeon, and C. Gale, *Phys. Rev. C* **82**, 014903 (2010).  
 [19] W. Israel, *Ann. Phys. (Leipzig)* **100**, 310 (1976).  
 [20] J. Stewart, *Proc. R. Soc. A* **357**, 59 (1977).  
 [21] W. Israel and J.M. Stewart, *Ann. Phys. (Leipzig)* **118**, 341 (1979).  
 [22] M. Grmela and H.C. Ottinger, *Phys. Rev. E* **56**, 6620 (1997).  
 [23] A. Muronga, *Phys. Rev. Lett.* **88**, 062302 (2002).  
 [24] R. Baier, P. Romatschke, D.T. Son, A.O. Starinets, and M.A. Stephanov, *J. High Energy Phys.* **04** (2008) 100.  
 [25] A. Kurganov and E. Tadmor, *J. Comput. Phys.* **160**, 241 (2000).  
 [26] R. Naidoo and S. Baboolal, *Future Gener. Comput. Syst.* **20**, 465 (2004).  
 [27] M.D. Duez *et al.*, *Phys. Rev. D* **69**, 104030 (2004).  
 [28] A.M. Poskanzer and S.A. Voloshin, *Phys. Rev. C* **58**, 1671 (1998).  
 [29] M.L. Miller, K. Reygers, S.J. Sanders, and P. Steinberg, *Annu. Rev. Nucl. Part. Sci.* **57**, 205 (2007).  
 [30] P. Jacobs, *Eur. Phys. J. C* **43**, 467 (2005).  
 [31] F. Wang, *J. Phys. G* **30**, S1299 (2004).  
 [32] J. Adams *et al.*, *Phys. Rev. Lett.* **95**, 152301 (2005).  
 [33] P. Huovinen and P. Petreczky, *Nucl. Phys. A* **837**, 26 (2010).  
 [34] K. Dusling, G.D. Moore, and D. Teaney, *Phys. Rev. C* **81**, 034907 (2010).  
 [35] V. Greco and C.M. Ko, *Phys. Rev. C* **70**, 024901 (2004).  
 [36] X. Dong *et al.*, *Phys. Lett. B* **597**, 328 (2004).  
 [37] J. Adams *et al.*, *Phys. Rev. C* **72**, 014904 (2005).  
 [38] A. Adare *et al.*, *Phys. Rev. Lett.* **105**, 062301 (2010).  
 [39] P. Romatschke and U. Romatschke, *Phys. Rev. Lett.* **99**, 172301 (2007).  
 [40] K. Dusling and D. Teaney, *Phys. Rev. C* **77**, 034905 (2008).  
 [41] D. Molnar and P. Huovinen, *J. Phys. G* **35**, 104125 (2008).  
 [42] H. Song and U. W. Heinz, *Phys. Rev. C* **78**, 024902 (2008).  
 [43] B.B. Back *et al.*, *Phys. Rev. C* **72**, 051901 (2005).  
 [44] P. Bozek and I. Wyskiel, *Proc. Sci.*, EPS-HEP-2009 (2009) 039.  
 [45] C. Nonaka and S.A. Bass, *Phys. Rev. C* **75**, 014902 (2007).  
 [46] P. Kovtun, D.T. Son, and A.O. Starinets, *Phys. Rev. Lett.* **94**, 111601 (2005).  
 [47] Z. Xu, C. Greiner, and H. Stoecker, *Phys. Rev. Lett.* **101**, 082302 (2008).